Available online at www.sciencedirect.com
ScienceDirect
Ceramics International 37 (2011) 2317–2322
CERAMICS INTERNATIONAL
www.elsevier.com/locate/ceramint

TBA-based freeze/gel casting of porous hydroxyapatite scaffolds

J.H. Kim [a], J.H. Lee [a], T.Y. Yang [a], S.Y. Yoon [a], B.K. Kim [b], H.C. Park [a,*]

[a] School of Materials Science and Engineering, Pusan National University, 30 Jangjeon-dong, Geumjeong-gu, Pusan 609-735, South Korea
[b] Department of Polymer Science and Engineering, Pusan National University, Pusan 609-735, South Korea

Received 26 January 2011; received in revised form 15 March 2011; accepted 15 March 2011
Available online 23 March 2011

Abstract

Porous ceramic scaffolds with a controlled ''designer'' pore structure have been prepared by the freeze/gel casting route using a TBA-based hydroxyapatite slurry system with 20–40 wt.% solid content. The products were characterized in terms of sintered microstructure, together with physical and mechanical properties. After sintering at 1050–1250 °C, the advantages of freeze casting and gel casting appeared in the pore structure and compressive strength of the ceramics, i.e., unidirectional aligned macro-pore channels developed by controlling the solidification direction of the TBA solvent used in the freeze casting together with small diameter (micron sized) isolated pores formed in the dense outer walls of the pore channels when processed by gel casting. The sintered porosity and pore size generally resulted in a high solid loading giving low porosity and small pore size, this leading to higher compressive strengths. The scaffolds obtained exhibited an average porosity and compressive strength in the range 41.9–79.3% and 35.1–2.7 MPa, respectively, depending on the processing conditions used.

Keywords: A. Sintering; B. Porosity; C. Strength; E. Biomedical application

1. Introduction

Tissue engineering scaffolds must satisfy biological (e.g., biocompatibility, bioactivity and osteoconductivity) and structural (e.g., 3-D interconnected pore structure and desirable pore size) requirements; the former is necessary for biological affinity with bone tissue, the latter for allowance of cell infiltration and host tissue growth in scaffolds [1,2]. Also, the scaffolds require high strength, sufficient to handle the unfired scaffold components and later after firing to support their skeleton structure in the initial stage of tissue attachment. Hydroxyapatite (HA) which has a similar chemical composition to the major inorganic component of natural bone is biocompatible as well as osteoconductive and is therefore widely used as a tissue scaffolding material [3–6]. The structural properties of scaffolds are mainly determined by the processing conditions; in this case the strategy has been to design novel pore microstructures together with a requirement for high strength.

Several processing techniques have been developed for fabricating porous bioceramic scaffolds, including replication of polymer foams [7–9], gel casting of foams [10,11] and thermal decomposition of volatile organic materials [12,13]. None of these methods can fully satisfy the characteristics required for totally acceptable scaffolds, namely a highly porous, large-sized (100–200 μm) pore structure having total interconnection combined with reasonable mechanical strength. For example, the sponge replica technique can give the desired porosity, the morphology consisting of highly interconnected and large-sized pores. However, the scaffolds obtained from this process generally exhibit poor mechanical strength, certainly not enough for load-bearing applications, mainly due to the reticulated skeletons which are often cracked during pyrolysis of the polymeric template [7,9,14]. Gel casting is used for fabricating ceramic scaffolds with relatively large-sized pores (i.e., of the order of several hundreds of micrometers) and also results in high mechanical strength. However, in this case the morphology of pores cannot routinely be controlled [15,16]. On the other hand, gel casting combined with a polymer sponge technique [17] has been introduced to produce porous HA scaffolds with large pore size (200–400 μm) and relatively high compressive yield strength

* Corresponding author. Tel.: +82 51 5102392; fax: +82 51 5120528.
E-mail address: hcpark1@pusan.ac.kr (H.C. Park).

0272-8842/$36.00
doi:10.1016/j.ceramint.2011.03.023

(~5 MPa with 71% porosity); however, any elaborate microstructural control could not be employed in this process.

Recently, freeze casting (freeze drying) has emerged as a promising process which can be used to prepare porous ceramic biomaterials. This simple process involves the preparation of a ceramic slip that is poured into a mold, it is then frozen and the suspension liquid sublimated away. The removal of frozen liquid by sublimation can lead to porous ceramics with uniquely shaped pore channel, e.g., long-range ordered and/or gradient pore structures. Deville [18] and Wegst et al. [19] have reviewed the processing, porous structure and properties of freeze-cast biomaterials, respectively. The porous structure is directly related to the solvent used and its solidification rate. Smaller pore size is commonly obtained with faster freezing rate. Camphene instead of water is widely used as the solvent to produce porous HA matrix scaffolds with a controlled pore structure [20–25]. The camphene-based freeze casting process is an effective process to give special porous structures (i.e., mainly consisting of dendrite-shaped pores) but it is very difficult to produce scaffolds which have sufficiently high porosity coincident with desirable mechanical strength.

In the present work, a freeze/gel casting technique has been utilized to prepare highly porous HA scaffolds with controlled microstructure and improved compressive strength, which are suitable for tissue engineering applications. In this processing route, tertiary-butyl alcohol (TBA) was selected as the freezing solvent, which can leave relatively long pore channels after removal of the alcohol by sublimation. This is the result of its preferential solidification, characteristically in a straight direction [26,27]. The resulting scaffolds were characterized in terms of crystalline phase, microstructure, physical and mechanical properties.

2. Experimental procedure

2.1. Materials

Commercially available HA powder ($Ca_{10}(PO_4)_6(OH)_2$) (Alfa Aesar) (Fig. 1) and reagent-grade TBA ($C_4H_{10}O$) (Junsei Chemical) were selected as the bioactive ceramic and the freezing vehicle, respectively. TBA-based freeze/gel-casting slurries were prepared using various processing additives: citric acid (Aldrich Chemical) dispersant; ethoxylated acetylenic diol (Dynol 604, Air Products and Chemicals) surfactant; reactive organic monomer gelators, i.e., mono-functional acrylamide (AM, $C_2H_3CONH_2$, Aldrich Chemical) and di-functional *N*,*N*′-methylenebisacrylamide (MBAM, $(C_2H_3CONH)_2CH_2$, Aldrich Chemical); free radical initiator, i.e., ammonium persulphate (APS, $(NH_4)_2S_2O_8$, Kanto Chemical).

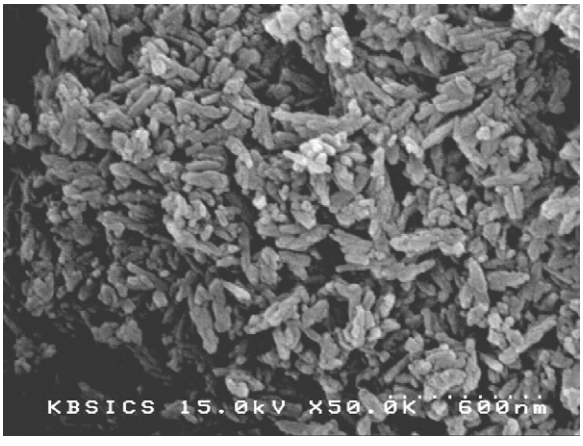

Fig. 1. Scanning electron micrograph of as-received HA powder.

2.2. Processing

The freeze/gel-casting slurries were prepared at 20, 30, and 40 wt.% solid loading by adding HA powder into premixed solution with TBA/AM/MBAM (wt.%) = 90/9.6/0.4; then, 1 wt.% citric acid, based on HA powder content and 0.25 wt.% Dynol 604, based on monomer solution were then added. The prepared slurries were homogenized by ball milling at 40 °C for 24 h and then stabilized at 30 °C in a water bath, followed by de-airing under vacuum for 3 min. For further polymerization of AM, an aqueous solution of 40 wt.% initiator APS, was slowly dropped into the slurries which were continuously stirred for 10 min at 40 °C using a magnetic stirrer. A 20 wt.% concentrated solution was used up to 40 wt.% solid loading to control the polymerization rate; the actual amount of initiator added was 2 wt.%, based on the monomer content.

The prepared warm HA slurry was then poured into the polyethylene cylindrical mold (30 mm in diameter). Subsequently, the mold was placed on a stainless steel plate which was temperature-controlled at <0 °C. Under these conditions, controlled freezing of the TBA gradually takes place from bottom to top of the specimen, resulting in unidirectional TBA solidification, which on its sublimation will give pore channels throughout the whole cast body. Subsequently, the TBA was sublimated in a freeze drier (Labconco 77540, Western Medics), resulting in the large longitudinal pore channels in a green body. After preliminary calcination at 600 °C for 1 h with a heating rate of 1 °C/min to remove organic additives, the samples were finally sintered at 1050–1250 °C for 2 h (heating rate: 3 °C/min) in air.

2.3. Characterization

The crystalline phase, morphology, porosity, and mechanical properties of the fabricated porous HA scaffolds were investigated and measured. The crystalline phase was examined using X-ray diffractometry (XRD, D/max-IIA, Rigaku). The pore and skeleton morphologies were observed using a scanning electron microscopy (SEM, JSA-840A, Jeol). The compressive strength in the direction parallel to the freezing direction was measured for five sintered samples with dimensions of 18 mm diameter x 12 mm height using a Universal Test Machine (model 6025, Instron) with a crosshead speed of 0.5 mm/min and a load cell of 1 kN. The sintered bulk density and porosity were measured by the water immersion method.

3. Results and discussion

3.1. Crystalline phases of sintered scaffolds

Crystalline phases of the sintered freeze/gel-cast scaffolds have been examined by XRD analysis; the XRD patterns of as-received HA powder and its sintered scaffolds are given in Fig. 2. After sintering at 1050–1250 °C for 2 h, nearly all characteristic peaks corresponding to HA (JCPDS card # 9-432) were confirmed to be present. The peak intensities in sintered materials were somewhat higher than those in as-received HA powder, due to the increase of HA crystallinity but they were scarcely changed with increasing sintering temperature. From the XRD results, it appears possible to sinter the scaffolds at temperatures ≤1250 °C without any loss of $(OH)^-$ groups in the HA.

3.2. Porous structures

The SEM micrographs of the cross-sections parallel and perpendicular to the macroscopic solidification direction of TBA solvent for sintered freeze/gel-cast scaffolds are shown in Figs. 3 and 4, respectively. The unidirectional pore channels aligned regularly along the growth direction of TBA solid were observed to extend over a long range (Fig. 3a); in addition, the walls of the pore channels were well connected to each other. Such morphology is clearly distinguished from the dendritic structure of water- or camphene-based freeze casting which grows in several directions [25,28]. The linear growth of the TBA solid over a considerable length at its freezing temperature after sublimation and sintering may more easily provide a pore channel suitable for blood supplies to the developing connective tissue.

At higher magnifications, the internal walls of the pore channels exhibited a porous structure (>8.3 μm in layer thickness); also, the porous structure was mainly composed of a high volume fraction of small sized pores (∼<1.2 μm) which are the traces of microscopic TBA solid (Fig. 3b). With increasing firing temperature up to 1250 °C, the structure became less porous through the densification and coalescence

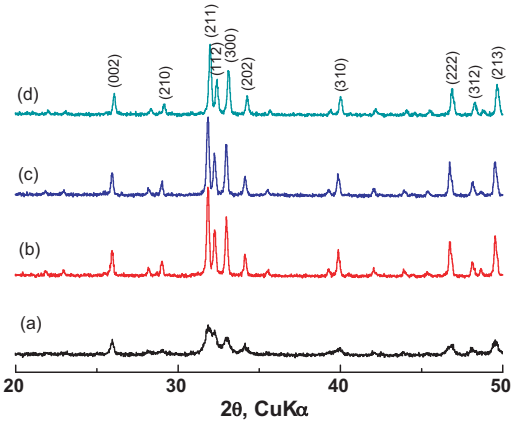

Fig. 2. XRD patterns of (a) as-received HA powder and porous HA scaffolds sintered at (b) 1050 °C, (c) 1150 °C and (d) 1250 °C for 2 h.

process of the initial particles; then, fine (<0.8 μm) intergranular pores formed. On the other hand, the outer walls of the pore channels showed a relatively dense structure (0.3–0.8 μm in layer thickness) which may consist of hard agglomerated crystals; especially, the degree of densification was further improved after sintering at 1250 °C (Fig. 3d).

From the observation of the microstructure of sintered scaffolds, consequently, it is considered that the two types of pores formed, i.e., large extended pore channels and micropores inside the walls are selectively determined by the spacing and morphology of the TBA solid structure formed during the freezing stage and removed during sublimation. Such a microstructure made up of the continuous scaffolds could give a respectable mechanical strength and at the same time allow re-growth mechanisms to take place via the controlled biomimetic porosity.

A similar porous structure consisting mainly of unidirectional pore channels was obtained (Fig. 4); however, the pore size was somewhat affected by processing variables. A small pore size and narrow pore size distribution (0.7–1.9 μm) were observed at high solid loading when compared to low solid loading (1.5–3.6 μm). After sintering at 1150 °C, the scaffolds with 20, 30 and 40 wt.% solid loading had an average pore size of ∼12.4, ∼10.1 and ∼5.3 μm, respectively. The average pore size (∼12.2 μm) of scaffolds obtained after sintering at 1050 °C with 30 wt.% solid loading is similar to that of scaffolds sintered at 1150 °C with 20 wt.% solid loading. Such a pore morphology and pore size can allow fibroblasts (5–15 μm) to grow into the scaffolds [29].

3.3. Properties of sintered scaffolds

After sintering at 1050–1250 °C, the porosity, shrinkage, bulk density and compressive strength of porous HA scaffolds fabricated with different solid loadings are given in Table 1. With increasing solid loading and sintering temperature, as might be expected, the apparent porosity (79.3–41.9%) decreased while the shrinkage (24.6–34.4%) in the direction perpendicular to the freezing direction increased, resulting in an increase in compressive strength (2.7–35.1 MPa). The compressive strength of almost all porous scaffolds fabricated is comparable to that (4–15 MPa) of cancellous bone [30]. The maximum compressive strength (35.1 MPa) was obtained in the porous HA scaffolds sintered at 1250 °C with 40 wt.% solid loading, presumably due to the smaller pore channels (3.7–7.4 μm) and denser wall structure (Fig. 5). Several studies on the compressive strength of freeze-cast HA scaffolds have been reported; however, in this case the direct comparison of compressive strength of the scaffolds is not reasonable because of their different porous structure. For example, Lee et al. [24] obtained highly porous ceramics with interconnected, dendrite-structured pore channels by camphene-based freeze casting of 10 vol.% HA slurries. After sintering at 1250 °C, the porosity and compressive strength were 75% and 0.94 MPa, respectively. Macchetta et al. [25] prepared HA/TCP composite scaffolds using a room temperature (4–30 °C) camphene-based freeze casting of 10 vol.% solid loading slurries which after

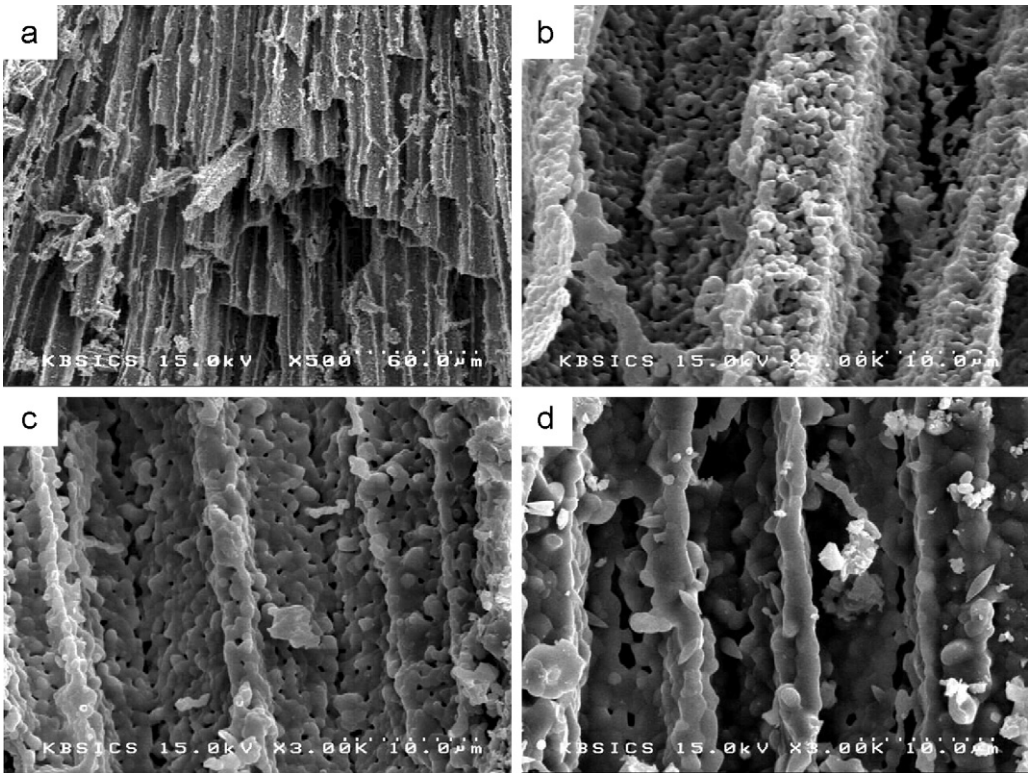

Fig. 3. Scanning electron micrographs of cross sections parallel to the macroscopic TBA ice growth direction; sintered at (a) 1150 °C with 20 vol.% solid loading, (b) 1050 °C with 30 wt.%, (c) 1150 °C with 30 wt.% and (d) 1250 °C with 30 wt.%.

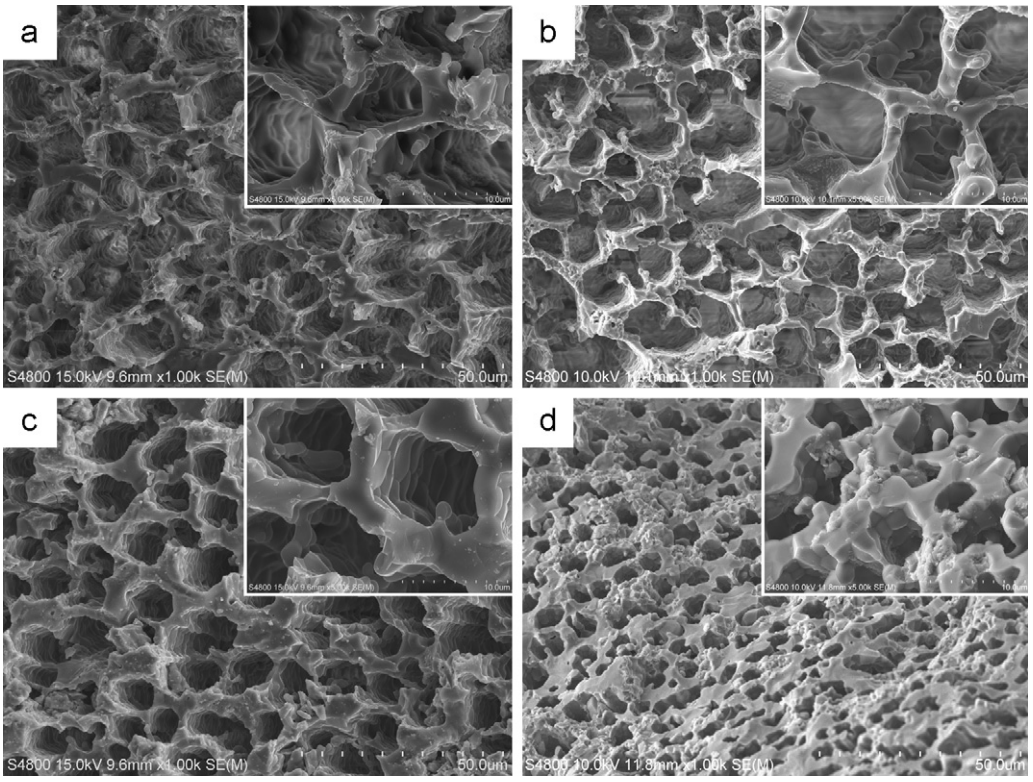

Fig. 4. Scanning electron micrographs of cross sections perpendicular to the macroscopic TBA ice growth direction; sintered at (a) 1050 °C with 30 wt.% solid loading, (b) 1150 °C with 20 wt.%, (c) 1150 °C with 30 wt.% and (d) 1150 °C with 40 wt.%.

Table 1
Porosity, shrinkage, bulk density and compressive strength of porous HA scaffolds obtained by sintering at 1050–1250 °C for 2 h with different solid loadings.

Sintering temperature (°C)	Solid loading (wt.%)	Porosity (%)	Linear shrinkage (%)	Bulk density (g/cm^3)	Compressive strength (MPa)
1050	20	79.3 ± 1.1	24.6	0.62	2.7 ± 0.8
	30	68.1 ± 2.3	25.4	0.92	7.2 ± 1.5
	40	57.0 ± 3.3	26.1	1.26	22.3 ± 0.8
1150	20	76.5 ± 1.2	28.2	0.71	5.7 ± 0.6
	30	64.6 ± 1.4	29.4	1.02	15.2 ± 1.0
	40	49.9 ± 3.6	30.3	1.46	27.8 ± 2.5
1250	20	67.0 ± 1.0	32.3	1.26	6.8 ± 0.7
	30	59.5 ± 4.0	33.3	1.46	17.3 ± 1.9
	40	41.9 ± 2.5	34.4	1.69	35.1 ± 2.9

sintering 1280 °C, gave a porous scaffold with large pore channels containing secondary dendrites. They found that on decreasing the freeze temperature from 30 °C to 4 °C, the compressive strength (72.5% porosity, 100–200 μm pore size) increased from 1.95 MPa to 2.98 MPa. Fu et al. [31] obtained lamellar-typed porous scaffolds by freeze casting of 20 vol.% aqueous HA suspension with the addition of 20 wt.% glycerol; after sintering at 1350 °C for 3 h, they had the maximum compressive strength of ∼18 MPa (46% porosity,) measured in the direction parallel to the freezing direction. Deville et al. [32] fabricated porous HA scaffolds having very high compressive strength of 65 MPa (56% porosity) by freeze casting (cooling rates: >5 °C/min) of aqueous slurries with 50 wt.% solid loading and then sintering at 1300 °C for 4 h. They concluded that this unusually high compressive strength is due to the dense, cellular and lamellar structure consisting of the processed scaffolds, which can clearly be divided into three distinct zones.

The compressive strength of porous scaffolds are influenced by many parameters, including porosity, pore shape, pore size, wall thickness and wall density, which are mainly determined by fabrication processes. However, it is difficult to take all the parameters into account since they are interdependent and the compressive strength is affected by all of them via the microstructure, especially in the case of sintering. Generally, among these parameters the compressive strength of porous materials influenced is primarily by the degree of porosity. In this study, therefore, the relationship between porosity and compressive strength was plotted and is given in Fig. 6. The compressive strength generally behaved in an inverse manner to the porosity, i.e., low porosity gave high compressive strength due to the high bulk density (shrinkage) of sintered materials (Table 1); in this case, a higher reliability of compressive strength could be seen in relatively more porous samples with low solid loading (20 wt.%) compared with high solid loading, probably due to a relatively uniform porosity. The linear relationship between compressive strength and porosity shown in Fig. 6 can be approximately expressed by the equation:

$$y = 70.02 - 0.85x \quad (1)$$

in which y is the compressive strength (MPa) and x is the porosity (%).

Clearly the properties of sintered scaffolds were affected by the processing variables (i.e., solid loading and sintering temperature), especially the level of solid loading. It is considered that since the scaffolds in tissue engineering require a high porosity (macro) for effective cell infiltration and host tissue intergrowth, as well as a high wall density (micro) for

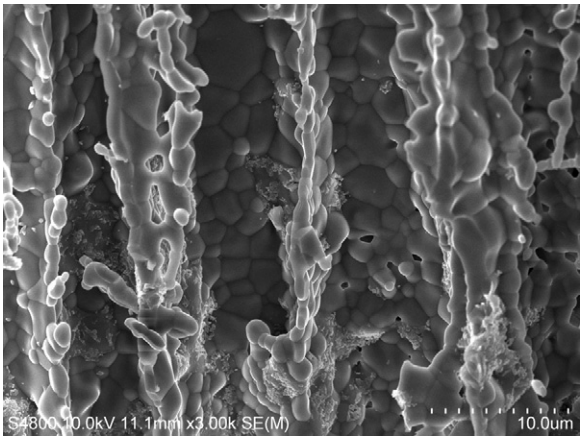

Fig. 5. Scanning electron micrographs of cross sections perpendicular to the macroscopic TBA ice growth direction; sintered at 1250 °C with 40 wt.% solid loading.

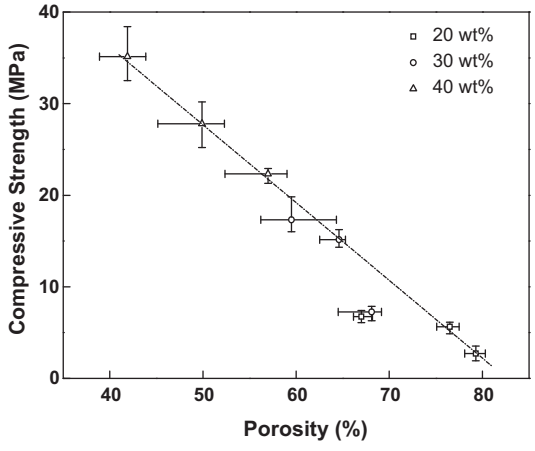

Fig. 6. The relationship between compressive strength and porosity in porous HA scaffolds sintered at 1050–1250 °C for 2 h.

high mechanical strength. Thus the optimum processing conditions corresponding to specific application for tissue substitution can be selected and produced in the form of designer microstructures.

4. Conclusions

Highly porous HA scaffolds with a unique pore structure and desirable compressive strength can be prepared by the controlled TBA-based freeze/gel-casting technique. The results indicate considerable promise for tissue engineering applications. The pore morphology of the scaffolds appears to be tailored by the control available in the freeze casting and gel casting stages, i.e., unidirectional pore channels (5.3–12.4 μm in diameter) with a long range by TBA-based freeze casting and dense walls with a few isolated, small-sized pores (<0.8 μm) by gel casting. With increasing solids loading from 20 wt.% to 40 wt.%, the sintered porosity (79.3–41.9%) and average pore size (12.4–5.3 μm) decreased, while the compressive strength (2.7–35.1 MPa) increased. Consequently, since a relatively wide-ranged pore size and compressive strength can be obtained using a combined processing route applied and furthermore the compressive strength is inversely proportional to the porosity, hence it becomes possible to select the optimum fabrication conditions corresponding to a specific requirement for particular application in tissue engineering.

Acknowledgements

This work was supported by National Research Foundation of Korea Grant Funded by the Korea Government (2010-0016401).

References

[1] K.J.L. Burg, S. Porter, J.F. Kellam, Biomaterial developments for bone tissue engineering, Biomaterials 21 (2000) 2347–2359.
[2] S.F. Hulbert, J.C. Bokros, L.L. Hench, J. Wilson, G. Heimke, Ceramics in clinical applications: past, present and future, in: P. Vincenzini (Ed.), High Tech Ceramics, Elsevier, Amsterdam, Netherlands, 1987, pp. 189–213.
[3] W. Suchanek, M. Yoshimura, Processing and properties of hydroxyapatite-based biomaterials for use as hard tissue replacement implants, J. Mater. Res. 13 (1998) 94–117.
[4] S. Padilla, S. Sanchez-Salcedo, M. Vallet-Regi, Bioactive and biocompatible pieces of HA/sol–gel glass mixtures obtained by the gel-casting method, J. Biomed. Mater. Res. 75A (2005) 63–72.
[5] L. Cerroni, R. Filocamo, M. Fabbri, C. Piconi, S. Caropreso, S.G. Condo, Growth of osteoblast-like cells on porous hydroxyapatite ceramics: an in vitro study, Biomol. Eng. 19 (2002) 119–124.
[6] L.L. Hench, J. Wilson, Surface-active biomaterials, Science 226 (1984) 630–636.
[7] I.K. Jun, J.H. Song, W.Y. Choi, Y.H. Koh, H.E. Kim, Porous hydroxyapatite scaffolds coated with bioactive apatite-wollastonite glass–ceramics, J. Am. Ceram. Soc. 90 (2007) 2703–2708.
[8] H.W. Kim, J.C. Knowles, H.E. Kim, Hydroxyapatite porous scaffold engineered with biological polymer hybrid coating for antibiotic vancomycin release, J. Mater. Sci. Mater. Med. 16 (2005) 189–195.
[9] Y. Zhang, M. Zhang, Three-dimensional macroporous calcium phosphate bioceramics with nested chitosan sponges for load bearing bone implants, J. Biomed. Mater. Res. A61 (2002) 1–8.
[10] F.Z. Zhang, T. Kato, M. Fuji, M. Takahashi, Gelcasting fabrication of porous ceramics using a continuous process, J. Eur. Ceram. Soc. 26 (2006) 667–671.
[11] J. Yang, H. Lin, X. Xi, K. Zeng, Porous ceramic from particle-stabilized foams via gelcasting, Int. J. Mater. Prod. Technol. 37 (2010) 248–256.
[12] S.W. Yook, H.E. Kim, B.H. Yoon, Y.M. Soon, Y.H. Koh, Improvement of compressive strength of porous hydroxyapatite scaffolds by adding polystyrene to camphene-based slurries, Mater. Lett. 63 (2009) 955–958.
[13] O. Lyckfeldt, J.M.F. Ferreira, Processing of porous ceramics by 'starch consolidation', J. Eur. Ceram. Soc. 18 (1998) 131–140.
[14] A.R. Studart, U.T. Gonzenbach, E. Tervoort, L.J. Gauckler, Processing routes to macroporous ceramics: a review, J. Am. Ceram. Soc. 89 (2006) 1771–1789.
[15] T.M.G. Chu, J.W. Halloran, S.J. Hollister, S.E. Feinberg, Hydroxyapatite implants with designed internal architecture, J. Mater. Sci. Med. 12 (2001) 471–478.
[16] P. Sepulveda, J.G.P. Binner, S.O. Rogero, O.Z. Higa, J.C. Bressiani, Production of porous hydroxyapatite by the gel casting of foams and cytotoxic evaluation, J. Biomed. Mater. Res. A50 (2000) 27–34.
[17] H.R. Ramay, M. Zhang, Preparation of porous hydroxyapatite scaffolds by combination of the gel-casting and polymer sponge methods, Biomaterials 24 (2003) 3293–3302.
[18] S. Deville, Freeze-casting of porous biomaterials: structure, properties and opportunities, Materials 3 (2010) 1913–1927.
[19] U.G.K. Wegst, M. Schecter, A.E. Donius, P.M. Hunger, Biomaterials by freeze casting, Phil. Trans. R. Soc. A 368 (2010) 2099–2121.
[20] B.H. Yoon, Y.H. Koh, C.S. Park, H.E. Kim, Generation of large pore channels for bone tissue engineering using camphene-based freeze casting, J. Am. Ceram. Soc. 90 (2007) 1744–1752.
[21] S.W. Yook, H.E. Kim, B.H. Yoon, Y.M. Soon, H.Y. Koh, Improvement of compressive strength of porous hydroxyapatite scaffolds by adding polystyrene to camphene-based slurries, Mater. Lett. 63 (2009) 955–958.
[22] B.H. Yoon, C.S. Park, H.E. Kim, Y.H. Koh, *In-situ* fabrication of porous hydroxyapatite (HA) scaffolds with dense shells by freezing HA/camphene slurries, Mater. Lett. 62 (2008) 1700–1703.
[23] Y.M. Soon, K.H. Shin, Y.H. Koh, J.H. Lee, H.E. Kim, Compressive strength and processing of camphene-based freeze cast calcium phosphate scaffolds with aligned pores, Mater. Lett. 63 (2009) 1548–1550.
[24] E.J. Lee, Y.H. Koh, B.H. Yoon, H.E. Kim, H.W. Kim, Highly porous hydroxyapatite bioceramics with interconnected pore channels using camphene-based freeze casting, Mater. Lett. 61 (2007) 2270–2273.
[25] A. Macchetta, I.G. Turner, C.R. Bowen, Fabrication of HA/TCP scaffolds with a graded and porous structure using a camphene-based freeze-casting method, Acta Biomater. 25 (2009) 1319–1327.
[26] R. Chen, C.A. Wang, Y. Huang, L. Ma, W. Lin, Ceramics with special porous structures fabricated by freeze-gelcasting: using tert-butyl alcohol as a template, J. Am. Ceram. Soc. 90 (2007) 3478–3484.
[27] R. Chen, Y. Huang, C.A. Wang, J. Qi, Ceramics with ultra-low density fabricated by gelcasting: an unconventional view, J. Am. Ceram. Soc. 90 (2007) 3424–3429.
[28] T. Fukasawa, M. Ando, Synthesis of porous ceramics with complex pore structure by freeze-dry processing, J. Am. Ceram. Soc. 84 (2001) 230–232.
[29] V.S. Komlev, S.M. Barinov, Porous hydroxyapatite ceramics of bi-modal pore size distribution, J. Mater. Sci. Mater. Med. 13 (2002) 295–299.
[30] S. Yang, K.F. Leong, Z. Du, C.K. Chua, The design of scaffolds for use in tissue engineering. Part I. Traditional factors, Tissue Eng. 7 (2001) 679–689.
[31] Q. Fu, M.N. Rahaman, F. Dogan, B.S. Bal, Freeze casting of porous hydroxyapatite scaffolds. II. Sintering, microstructure, and mechanical behavior, J. Biomed. Mater. Res. Part B 86B (2008) 514–522.
[32] S. Deville, E. Saiz, A.P. Tomsia, Biomaterials 27 (2006) 5480–5489.